Published in final edited form as:
J Comput Assist Tomogr. 2012 January ; 36(1): 83–87. doi:10.1097/RCT.0b013e31824258cb.

"Sweet spot" for endoleak detection: Optimizing contrast to noise using low keV reconstructions from fast-switch kVp dual energy CT

Katherine E Maturen, MD,
University of Michigan Hospitals, Department of Radiology UH B1D530H, 1500 E Medical Center Drive, Ann Arbor MI 48109-5030, Phone (734) 232-6044, Fax (734) 615-1276, kmaturen@umich.edu

Ravi K Kaza, MD,
University of Michigan Hospitals, Department of Radiology TC B1132, 1500 E Medical Center Dr, Ann Arbor, MI 48109-5030, ravikaza@med.umich.edu

Peter S Liu, MD,
University of Michigan Hospitals, Department of Radiology UH B2A209, 1500 E Medical Center Dr, Ann Arbor, MI 48109-5030, peterliu@med.umich.edu

Leslie E Quint, MD,
University of Michigan Hospitals, Department of Radiology UH B1D530F, 1500 E Medical Center Drive, Ann Arbor MI 48109-5030, lequint@med.umich.edu

Shokoufeh H Khalatbari, MS, and
Michigan Inst. of Clinical and Health Research, 24 Frank Lloyd Wright, Lobby M 5738, Ann Arbor, MI 48109, skhalat@med.umich.edu

Joel F Platt, MD
University of Michigan Hospitals, Department of Radiology UH B1D502, 1500 E Medical Center Drive, Ann Arbor MI 48109-5030, jplatt@med.umich.edu

Abstract

Objective—To assess endoleak detection and conspicuity using low keV monochromatic reconstructions of single source (fast-switch kVp) dual energy datasets.

Methods—With IRB approval, multiphasic dual energy CT scans for aortic endograft surveillance were retrospectively reviewed for 39 patients. Two abdominal radiologists each performed two separate reading sessions, at 55 keV and standard 75 keV reconstruction, respectively. Readers tabulated endoleak presence, conspicuity on 1-5 scale, and type overall and in arterial and venous phases. Originally dictated reports in medical records were used as gold standard.

Results—Original dictations identified 19 endoleaks (9 abdominal and 10 thoracic), 13 of which were Type II. The blinded readers (R1 and R2) exhibited good to very good intraobserver and interobserver agreement. Endoleak detection was higher at 55 keV than 75 keV (sensitivity 100% (CI 82.4-100.0%) and 84.2% (CI 60.4-96.6%)at 55 keV vs. 79% (CI 54.4-94.0%)and 68.4% (CI 43.5-87.4%) at 75 keV in venous phase). Further, endoleak conspicuity ratings (where original dictation showed positive leak) were higher at 55 keV than 75 keV, which was a significant difference for R2 in the overall ratings (p=.03) and for both readers in the venous phase ratings

Correspondence to: Katherine E Maturen.

(R1:p=.01; R2: p=.004). There was no difference in endoleak type characterization between the keV levels.

Conclusion—Sensitivity for endoleak detection and overall endoleak conspicuity ratings were both higher at 55 keV than 75 keV, favoring the inclusion of a lower energy monochromatic reconstruction for endoleak surveillance protocols with dual energy CT.

Keywords

dual energy CT; endoleak detection; low kVp CT; aorta; endograft surveillance

Introduction

Patients undergoing aortic endograft repair of their abdominal or thoracic aneurysms are typically subject to lifelong annual imaging surveillance [1]. Although the optimal imaging protocol remains an area of active research [2-8], in many institutions a multiphasic CT scan is performed [9-11]. Improved endoleak detection in any one phase could simplify protocols and reduce radiation exposure.

The diagnosis of an endoleak requires detection of iodine, in the form of a pool of iodinated contrast-opacified blood within the excluded aneurysm sac. For any imaged material, radiographic conspicuity peaks at a photon energy (keV) level just above the outer shell binding energy (K –edge) of that material [12]. At this point the probability of the photoelectric effect greatly exceeds that of Compton scatter, resulting in greater image contrast [12]. The K-edge of iodine is 33.2 keV, meaning that in the lower diagnostic photon energy range, iodine looks brighter. However, image noise is also greater at lower keV [13], and these two factors must be balanced to optimize detection of endoleaks.

Low kVp and dual-energy CT can exploit the K-edge phenomenon to improve soft tissue contrast and diagnostic accuracy [14]. Fast-switch kVp is a specific dual energy CT technology with two rapidly alternating beams (usually at 80 and 140 kVp) from a single source. The x-ray tube alternates between 80 kVp and 140 kVp in about 0.5 milli-seconds at a constant tube current of approximately 600 mA to obtain adequately co-registered dual-energy projections. The exposure time ratio between the 80 kVp and 140 kVp scans is adjusted to 65:35 to account for the higher tube output at 140 kVp and to maximize contrast-to-noise ratio[15]. The energy separation of the two acquisitions allows for material decomposition analysis (prior to image reconstruction), a mathematical expression of any material's mass attenuation coefficient as a linear combination of any two "basis" materials exhibiting known changes in attenuation over the energy spectrum. Attenuation coefficients for each material are derived at each energy level and used to generate "monochromatic" single-keV images at any specific energy level between 40 and 140 keV, with less image noise than a single energy polychromatic acquisition at any particular kVp [16]. A 75 keV monochromatic series is typically reconstructed for clinical interpretation of dual energy datasets; this approximates a typical 120 kVp single energy CT acquisition and provides the best overall contrast to noise ratio [17] . However, specific imaging indications such as endoleak detection may be optimized at other energy levels. One of the potential benefits of dual energy CT is the ability to retrospectively manipulate the scan data in an effort to identify these nodal points:where image contrast and noise are in optimal balance.

Thus, using fast-switch kVp dual energy CT, the purpose of this study was to determine a useful keV level for endoleak detection then assess endoleak detection and subjective endoleak conspicuity at this level compared with standard 75 keV reconstructions.

Materials and Methods

Patients

IRB approval was obtained for a retrospective review of all DECT examinations during the first year of this technology at our institution (November 2009-November 2010). 108 post-endograft aortic CT scans were performed in 97 patients (28 women, 69 men), average age 72 (range 56-93). Among the 97 patients, 72 endografts were abdominal and 25 were thoracic. A subset of cases was selected for this pilot study; one non-blinded author identified a set of 40 cases to provide a mixture of exams in the chest and abdomen, with half positive for endoleak and half negative according to originally dictated reports. Blinded readers were not aware of the prevalence of endoleaks in the case set.

One of the 40 cases in the set was later excluded due to incomplete image capture on the radiology archive. 39 cases remained, 19 of which were interpreted as positive for endoleak according to original dictation. Among the 39 patients, 19 had abdominal endografts and 20 had thoracic endografts. The patient population included 14 women and 25 men, average age 75.6 years (range 56-93).

Scan technique

Endograft followup is routinely performed with triphasic technique at our institution. Dual energy CT protocol consisted of: pre-contrast (single energy) and arterial and venous post-contrast (both dual energy using fast-switch kVp) scans on GE HD-750 64-detector scanners (GE Healthcare, Milwaukee WI). Pre-contrast images were obtained with pitch 1.375:1, 100-120kVp; Auto mA 100/120 (min/max); 5 mm slice thickness. Injected contrast material was 120 cc iopamidol (Isovue-370, Bracco Diagnostics, Princeton NJ) at a rate of 4 cc/sec followed by 50 cc saline at the same rate. Arterial phase images were performed through entire abdomen and pelvis (with or without chest) at 150 HU aortic enhancement threshold using Smart Prep (GE Healthcare) bolus timing software (with region of interest in the proximal descending thoracic aorta for chest/abdomen/pelvis scans and in the upper abdominal aorta at the level of celiac axis for abdomen/pelvis only) and venous phase images obtained through region of endograft only at scan delay of 60 seconds after completion of arterial phase. Arterial and venous phase images were obtained with dual energy preset mA 600 and fast switch kVp from 80-140 kVp; arterial phase images reconstructed with 0.625 mm and venous phase images with 2.5 mm slice thickness.

Image processing and interpretation

The “Optimal CNR” (contrast to noise ratio) tool in the Gemstone Spectral Imaging (GSI) software package (GE Healthcare) was employed to analyze endoleak characteristics and guide experimental design. One non-blinded author placed regions of interest (ROIs) in each endoleak and within the excluded aneurysm sac, with automated generation of curves across the imaged energy spectrum (40-140 keV) and identification of the “Optimal CNR” keV level for each endoleak (Figures 1 and 2). “Optimal CNR” analysis of the endoleaks demonstrated average peak conspicuity level at 51.5 keV (range 48-54) in the arterial phase and 51.2 keV (range 49-56) in the venous phase. Based on these results, viewing levels of 55 keV and 75 keV were selected for comparison in this study.

Two authors (abdominal radiologists with 8 and 25 years post-residency experience repsectively) each performed two separate reading sessions (one at 55 and one at 75 keV), separated by more than two weeks. The readers generated each monochromatic series for interpretation at the GE Advantage Workstation with GSI (Gemstone Spectral Imaging, GE Healthcare) software at the time of interpretation. This process takes less than a minute. Readers had access to all phases of enhancement and ability to perform three dimensional

reconstructions but they did not have access to the original dictations or to reconstructions at other energy levels. The readers tabulated endoleak conspicuity on a 1-5 scale, ranging from (1) "No endoleak" to (5) "Definite endoleak". Ratings were recorded for the triphasic study overall and for each phase (arterial and venous) separately. Ratings of 4 and 5 were considered positive for endoleak, for purposes of statistical analysis. Endoleak type was also recorded, in accordance with standard reporting practices[18]. Because Type II endoleaks (lower pressure leaks arising from collateral vessels) are generally distinct from high pressure leaks in terms of clinical urgency[19], endoleaks were dichotomized into Type II and non-Type II for this small study.

The originally dictated radiology reports were used as the gold standard for interpretation. These had been rendered on the routine clinical PACS at standard 75 keV reconstruction levels for the dual energy components of the exam, with access to all phases of enhancement. Although the GE Advantage Workstation with GSI (Gemstone Spectral Imaging, GE Healthcare) software was in the reading room at the time of original interpretations, advanced post-processing was not part of routine clinical workflow.

Statistical analysis

Continuous variables were summarized using means and standard deviations. Kappa statistics were calculated for assessment of inter and intraobserver agreement for endoleak ratings. Prevalence-adjusted, bias-adjusted kappa (PABAK) was used to assess agreement for endoleak type due to the high prevalence of type II endoleaks. Reader ratings were compared with original dictations; sensitivity and specificity for endoleak detection were calculated with 95% confidence intervals. Wilcoxon signed rank test was used to test the significance of endoleak ratings between the two keV levels for each reader (where original dictation showed positive leak). A probability (p) value of 0.05 or smaller was considered significant for all hypothesis tests. The above procedures were performed using SAS 9.2 (SAS Institute, Cary NC).

Results

Intraobserver agreement was good to very good between phases at each keV level (Reader 1 kappa .64-.68; Reader 2 kappa .59-.67) and keV levels, overall and in each phase (Reader 1 kappa .79-.95; Reader 2 kappa .84-1.00). Reader interobserver agreement was also very good, overall and in each phase (Reader 1 vs. Reader 2 kappa .85-1.0 at 55 keV and .78-.94 at 75 keV). Sensitivity for endoleak detection was greater at 55 keV than 75 keV, presented in Table 1. These differences were noted in the overall and venous phase ratings. Specificity for endoleak detection was 100% for both readers at both keV levels. For studies rated positive for endoleak by original dictation (n=19), reader ratings of endoleak conspicuity were higher at 55 keV than 75 keV, as enumerated in Table 2. These differences were statistically significant for Reader 2 in the overall ratings and both readers in the venous phase ratings.

Regarding endoleak characterization, endoleaks were dichotomized into Type II and non-Type II. PABAK showed very good intraobserver agreement between keV levels for endoleak characterization (Reader 1 PABAK .88; Reader 2 PABAK .78) and good interobserver agreement (Reader 1 vs. Reader 2 kappa .65 at 55 keV and .63 at 75 keV). Reader sensitivity for Type II leak detection was similar at both keV levels (Reader 1 100% (CI 73.5-100%) at 55 keV and 100% (CI 73.5-100%) at 75 keV; Reader 2 100% (CI 73.5-100%) at 55 keV and 83.3% (CI 51.6-97.9%) at 75 keV).

Discussion

In this study, reader sensitivity for endoleak detection and subjective assessment of endoleak conspicuity were both higherin 55 keV than 75 keV images (the standard reconstruction that approximates a 120 kVp acquisition). This finding is in accordance with principles of imaging physics, given the proximity of the lower keV level to the K-edge of iodine[20]. The benefit of dual energy CT technique in this experimental design is twofold: the ability to generate low keV diagnostic images (analogous to a single energy low kVp acquisition), and the flexibility to retrospectively test conspicuity anywhere on the energy spectrum.

Theoretically, the lowest energy levels would yield the "brightest" iodine and the greatest image contrast, but the degree of noise at the low end of the diagnostic energy spectrum degrades these gains in contrast resolution. Thus, diagnosis-specific analysis may be needed to determine the best acquisition and viewing parameters for the many emerging applications of dual-energy and low-kVp CT, just as we employ specific window and level settings for particular indications. For example, 80 kVp imaging has been shown to increase the conspicuity of hypovascular pancreatic masses [21, 22], hypovascular[23] and hypervascular[24] liver lesions. These early studies have not yet demonstrated an improvement in lesion detection, nor has a specific ideal energy level been precisely set for each indication. Nonetheless a trajectory towards a more flexible and tissue-specific use of CT data has been established. It should also be noted that when "optimal" energy levels for this and other indications are experimentally demonstrated, low kVp single energy CT acquisition should confer the same diagnostic benefit as low keV dual energy CT reconstruction.

Several prior studies have assessed dual energy CT for endograft surveillance [25-28], but were focused primarily on the issue of iodine subtraction for virtual non-contrast imaging--and in one case the utility of iodine overlay techniques [28]--rather than testing endoleak conspicuity at various kVp levels. These studies employed dual source dual energy CT systems that did not at that time allow the flexibility of monochromatic (single energy) reconstructions at any energy level, as can be performed with single source (fast-switch kVp) systems. However, among this group of prior studies, Chandarana et al. [26] did note higher attenuation of endoleaks at the 80 kVp acquisition level than the weighted average or 140 kVp series. 80 kVp imaging has also been compared with 120 kVp protocols in normal-weight patients in other areas of vascular imaging [29-31], with the goals of establishing diagnostic adequacy, reducing radiation dose, or reducing contrast volume, rather than enhancing diagnostic accuracy.

Our results suggest that beyond adequacy, lower keV monochromatic reconstruction (and by inference lower kVp acquisition) actually improves diagnostic accuracy for endoleak detection. At the same time, dual energy technique has the potential to reduce patient dose (compared to multiphasic single energy CT acquisition) by substituting the virtual non-contrast series for a true non-contrast acquisition [25-27]. Specifically, our own comparison of dual energy and single energy scans for endograft surveillance found triphasic single energy scans had estimated effective doses in the range of 30-35 mSv compared with 20-25 mSv for biphasic dual energy scans (substituting virtual for true noncontrast series)[32]. Finally, most endoleaks are seen in the venous phase of enhancement [33]. Our results indicate that the alteration of viewing keV level has the greatest effect in the venous phase, which may embolden radiologists to drop the arterial phase from their protocols. The combination of these factors has great potential benefit for the thousands of patients undergoing annual imaging surveillance for endografts.

This retrospective study has several limitations, including the absence of angiographic proof of CT findings and the use of the originally dictated report as the gold standard. A subset of cases were selected for analysis in this pilot study, which may have altered the prevalence of endoleaks and introduced other biases. Only two kVp levels were tested; future research to establish the optimum viewing levels for this and other pathologies might test multiple levels in an effort to determine more precisely the threshold where noise overwhelms iodine conspicuity.

In summary, our initial experience with fast-switch kVp dual energy CT for endograft surveillance demonstrated both greater sensitivity for endoleak detection and higher conspicuity of endoleaks at 55 keV compared with the standard 75 keV reconstruction. We conclude that a lower energy reconstruction should be a routine part of dual energy CT protocols for this indication.

References

1. Prinssen M, Wixon CL, Buskens E, et al. Surveillance after endovascular aneurysm repair: diagnostics, complications, and associated costs. Ann Vasc Surg. 2004; 18:421–7. [PubMed: 15108054]
2. Black SA, Carrell TWG, Bell RE, et al. Long-term surveillance with computed tomography after endovascular aneurysm repair may not be justified. British journal of surgery. 2009; 96:1280–1283. [PubMed: 19847868]
3. Bley T, Chase P, Reeder S, et al. Endovascular abdominal aortic aneurysm repair: nonenhanced volumetric CT for follow-up. Radiology. 2009; 253:253–262. [PubMed: 19703867]
4. Wieners G, Meyer F, Halloul Z, et al. Detection of type II endoleak after endovascular aortic repair: comparison between magnetic resonance angiography and blood-pool contrast agent and dual-phase computed tomography angiography. Cardiovascular and interventional radiology. 2010; 33:1135–1142. [PubMed: 20924762]
5. Chaer R, Gushchin A, Rhee R, et al. Duplex ultrasound as the sole long-term surveillance method post-endovascular aneurysm repair: a safe alternative for stable aneurysms. Journal of vascular surgery. 2009; 49:845–9. [PubMed: 19341877]
6. van der Laan MJ, Bartels LW, Viergever MA, et al. Computed tomography versus magnetic resonance imaging of endoleaks after EVAR. European journal of vascular and endovascular surgery. 2006; 32:361–365. [PubMed: 16630731]
7. Harrison GJ, Oshin OA, Vallabhaneni SR, et al. Surveillance after EVAR Based on Duplex Ultrasound and Abdominal Radiography. European journal of vascular and endovascular surgery. 2011 In Press, Corrected Proof.
8. Verhoeven ELG, Oikonomou K, Ventin FC, et al. Is it time to eliminate CT after EVAR as routine follow-up? Journal of Cardiovascular Surgery. 2011; 52:193–198. [PubMed: 21460769]
9. Bean M, Johnson P, Roseborough G, et al. Thoracic aortic stent-grafts: utility of multidetector CT for pre- and postprocedure evaluation. Radiographics. 2008; 28:1835–1851. [PubMed: 19001643]
10. Hellinger J. Endovascular repair of thoracic and abdominal aortic aneurysms: pre-and postprocedural imaging. Techniques in vascular and interventional radiology. 2005; 8:2–15. [PubMed: 16098932]
11. Iezzi R, Cotroneo A, Filippone A, et al. Multidetector-row computed tomography angiography in abdominal aortic aneurysm treated with endovascular repair: evaluation of optimal timing of delayed phase imaging for the detection of low-flow endoleaks. Journal of computer assisted tomography. 2008; 32:609–615. [PubMed: 18664850]
12. Bushberg, J.; Seibert, J.; Leidholdt, E., et al. The Essential Physics of Medical Imaging. Philadelphia, PA: Lippincott Williams and Wilkins; 2002.
13. Yeh B, Shepherd J, Wang Z, et al. Dual-energy and low-kVp CT in the abdomen. AJR, American journal of roentgenology. 2009; 193:47–54. [PubMed: 19542394]

14. Coursey C, Nelson R, Boll D, et al. Dual-energy multidetector CT: how does it work, what can it tell us, and when can we use it in abdominopelvic imaging? Radiographics. 2010; 30:1037–1055. [PubMed: 20631367]
15. Li, B.; Yadeva, G.; Hsieh, J., et al. Head and body CTDI of dual-energy x-ray CT with fast-kVp switching. In: Sameh, E.; Pelc, N., editors. Medical Imaging 2010: Physics of Medical Imaging. Proceedings of SPIE; 2010.
16. Wu, X.; Langan, D.; Xu, D., et al. Monochromatic CT image representation via fast switching dual kVp. In: Samei, E.; H, J., editors. SPIE. 2009.
17. Zou, Y.; Silver, MD. Analysis of fast kV-switching in dual energy CT using a pre-reconstruction decomposition technique. In: Hsieh, J.; E, S., editors. SPIE. 2008.
18. Chaikof EL, Blankensteijn JD, Harris PL, et al. Reporting standards for endovascular aortic aneurysm repair. J Vasc Surg. 2002; 35:1048–60. [PubMed: 12021727]
19. Cao P, De Rango P, Verzini F, et al. Endoleak after endovascular aortic repair: classification, diagnosis and management following endovascular thoracic and abdominal aortic repair. J Cardiovasc Surg (Torino). 2010; 51:53–69.
20. Kalva S, Sahani D, Hahn P, et al. Using the K-edge to improve contrast conspicuity and to lower radiation dose with a 16-MDCT: a phantom and human study. Journal of computer assisted tomography. 2006; 30:391–397. [PubMed: 16778612]
21. Marin D, Nelson R, Barnhart H, et al. Detection of pancreatic tumors, image quality, and radiation dose during the pancreatic parenchymal phase: effect of a low-tube-voltage, high-tube-current CT technique--preliminary results. Radiology. 2010; 256:450–459. [PubMed: 20656835]
22. Macari M, Spieler B, Kim D, et al. Dual-source dual-energy MDCT of pancreatic adenocarcinoma: initial observations with data generated at 80 kVp and at simulated weighted-average 120 kVp. AJR, American journal of roentgenology. 2010; 194:W27–W32. [PubMed: 20028887]
23. Robinson E, Babb J, Chandarana H, et al. Dual source dual energy MDCT: comparison of 80 kVp and weighted average 120 kVp data for conspicuity of hypo-vascular liver metastases. Investigative radiology. 2010; 45:413–418. [PubMed: 20458250]
24. Altenbernd J, Heusner T, Ringelstein A, et al. Dual-energy-CT of hypervascular liver lesions in patients with HCC: investigation of image quality and sensitivity. European radiology. 2011; 21:738–743. [PubMed: 20936520]
25. Stolzmann P, Frauenfelder T, Pfammatter T, et al. Endoleaks after endovascular abdominal aortic aneurysm repair: detection with dual-energy dual-source CT. Radiology. 2008; 249:682–91. [PubMed: 18780822]
26. Chandarana H, Godoy MC, Vlahos I, et al. Abdominal aorta: evaluation with dual-source dual-energy multidetector CT after endovascular repair of aneurysms--initial observations. Radiology. 2008; 249:692–700. [PubMed: 18812561]
27. Sommer WH, Graser A, Becker CR, et al. Image quality of virtual noncontrast images derived from dual-energy CT angiography after endovascular aneurysm repair. J Vasc Interv Radiol. 2010; 21:315–21. [PubMed: 20097097]
28. Ascenti G, Mazziotti S, Lamberto S, et al. Dual-Energy CT for Detection of Endoleaks After Endovascular Abdominal Aneurysm Repair: Usefulness of Colored Iodine Overlay. AJR Am J Roentgenol. 2011; 196:1408–14. [PubMed: 21606306]
29. Sahani D, Kalva S, Hahn P, et al. 16-MDCT angiography in living kidney donors at various tube potentials: impact on image quality and radiation dose. AJR, American journal of roentgenology. 2007; 188:115–120. [PubMed: 17179353]
30. Schindera S, Graca P, Patak M, et al. Thoracoabdominal-aortoiliac multidetector-row CT angiography at 80 and 100 kVp: assessment of image quality and radiation dose. Investigative radiology. 2009; 44:650–655. [PubMed: 19724236]
31. Szucs Farkas Z, Schaller C, Bensler S, et al. Detection of pulmonary emboli with CT angiography at reduced radiation exposure and contrast material volume: comparison of 80 kVp and 120 kVp protocols in a matched cohort. Investigative radiology. 2009; 44:793–799. [PubMed: 19884825]
32. Maturen K, Kleaveland P, Kaza R, et al. Aortic endograft surveillance: Utility of fast-switch kVp dual energy CT with virtual non-contrast imaging. Journal of computer assisted tomography. 2012 Accepted for publication.

33. Macari M, Chandarana H, Schmidt B, et al. Abdominal aortic aneurysm: can the arterial phase at CT evaluation after endovascular repair be eliminated to reduce radiation dose? Radiology. 2006; 241:908–14. [PubMed: 17065562]

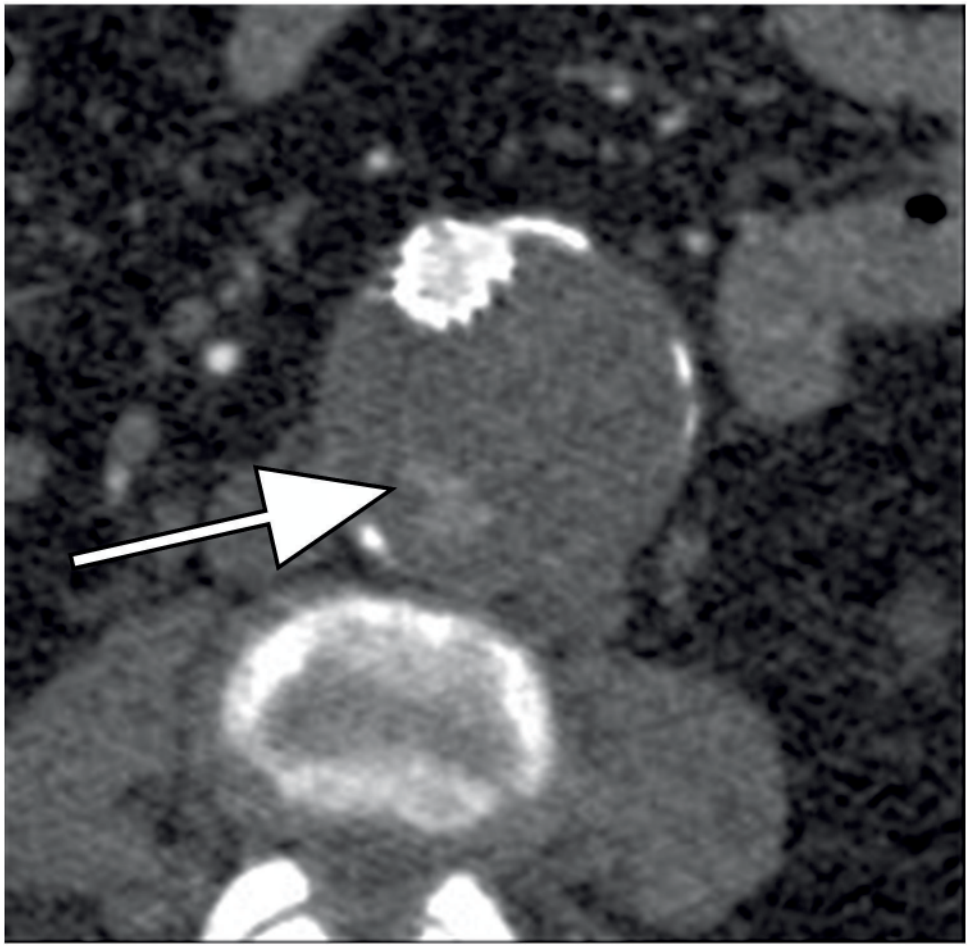

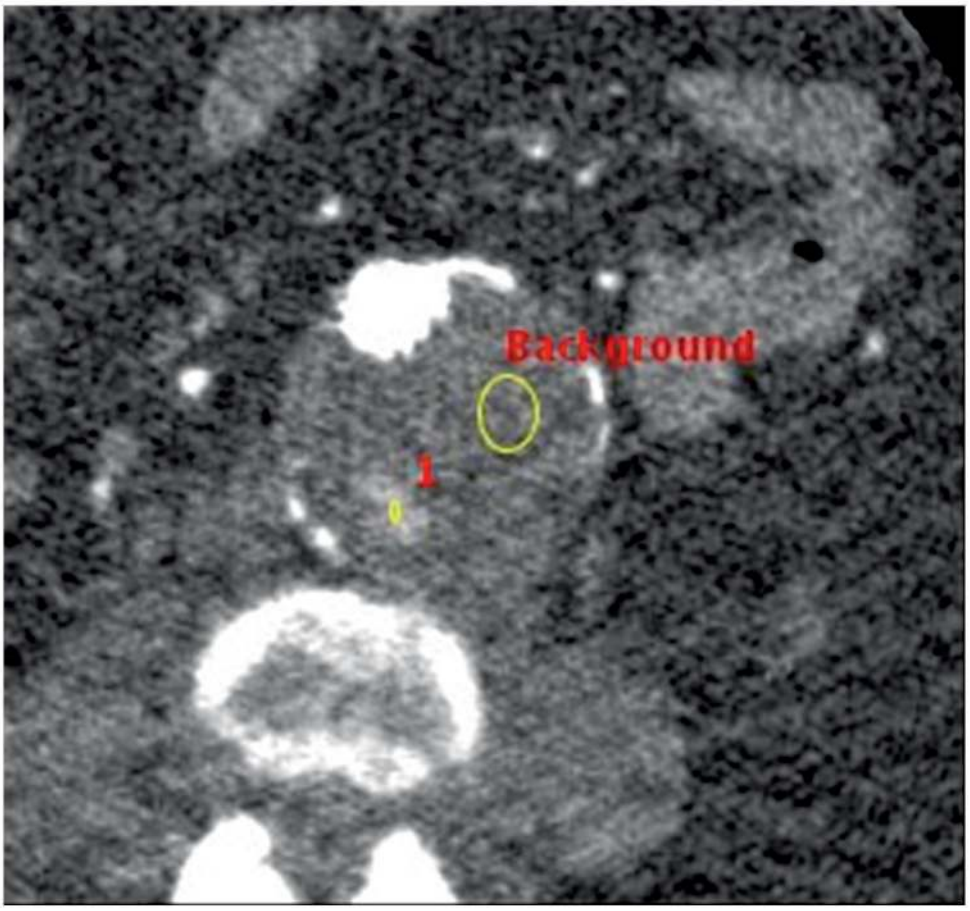

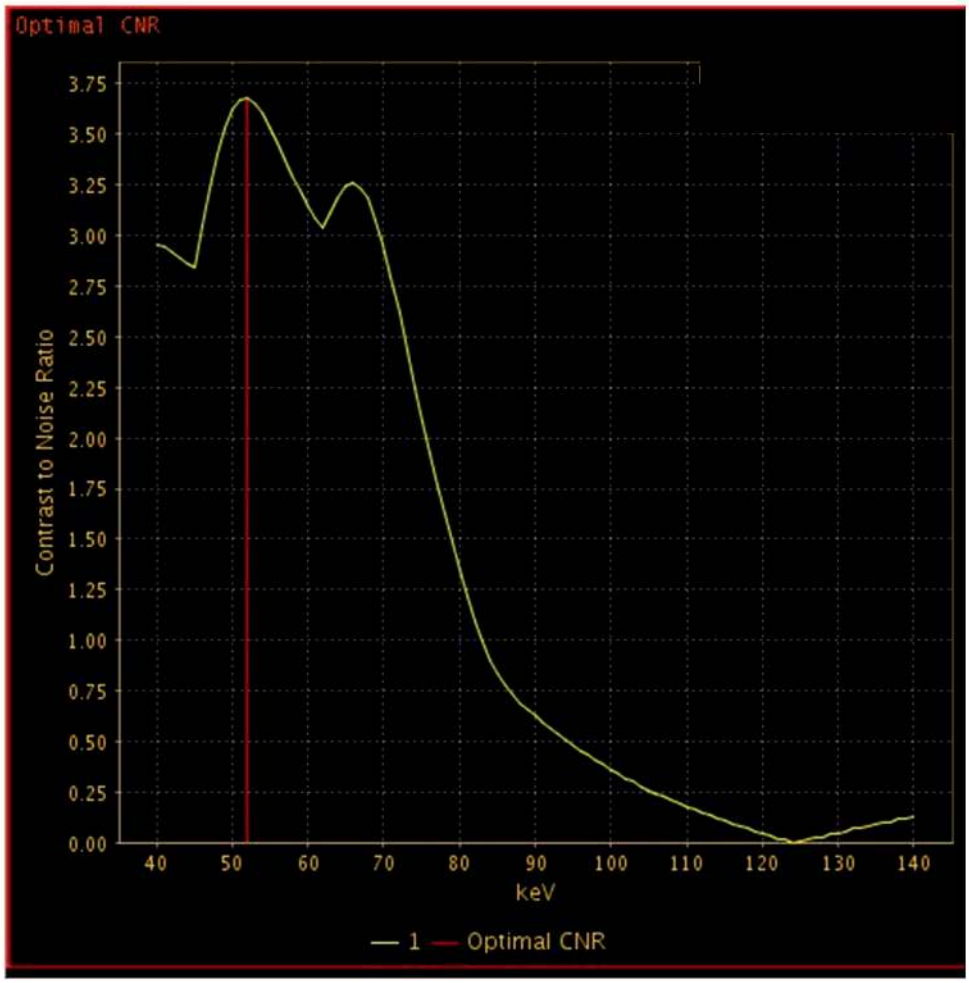

Figure 1.

77 year old woman with Type II endoleak associated with a lumbar artery.

A) Arterial phase CT image demonstrates focal contrast opacification (arrow) within the excluded aneurysm sac, compatible with endoleak.

B) Regions of interest placed on endoleak (labeled "1") and in thrombosed aneurysm sac (labeled "Background").

C) Optimal contrast-to-noise ratio (CNR) curve generated with Gemstone Spectral Imaging (GSI) software package (GE Healthcare) using above regions of interest for this specific endoleak, indicating maximum conspicuity at 54 keV (red vertical bar). A second slightly lower peak is noted around 70 keV in this and every patient, corresponding to the general peak of contrast-to-noise for monochromatic reconstructions from fast-switch kVp dual energy data.

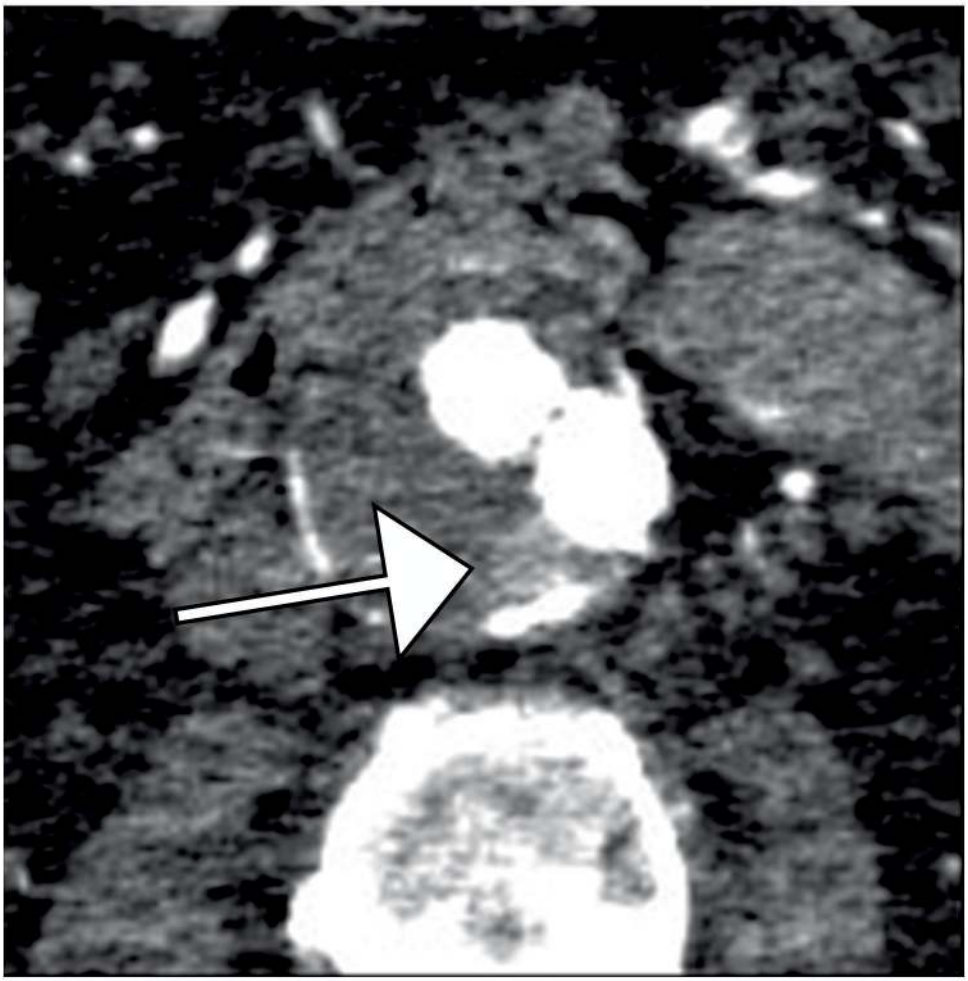

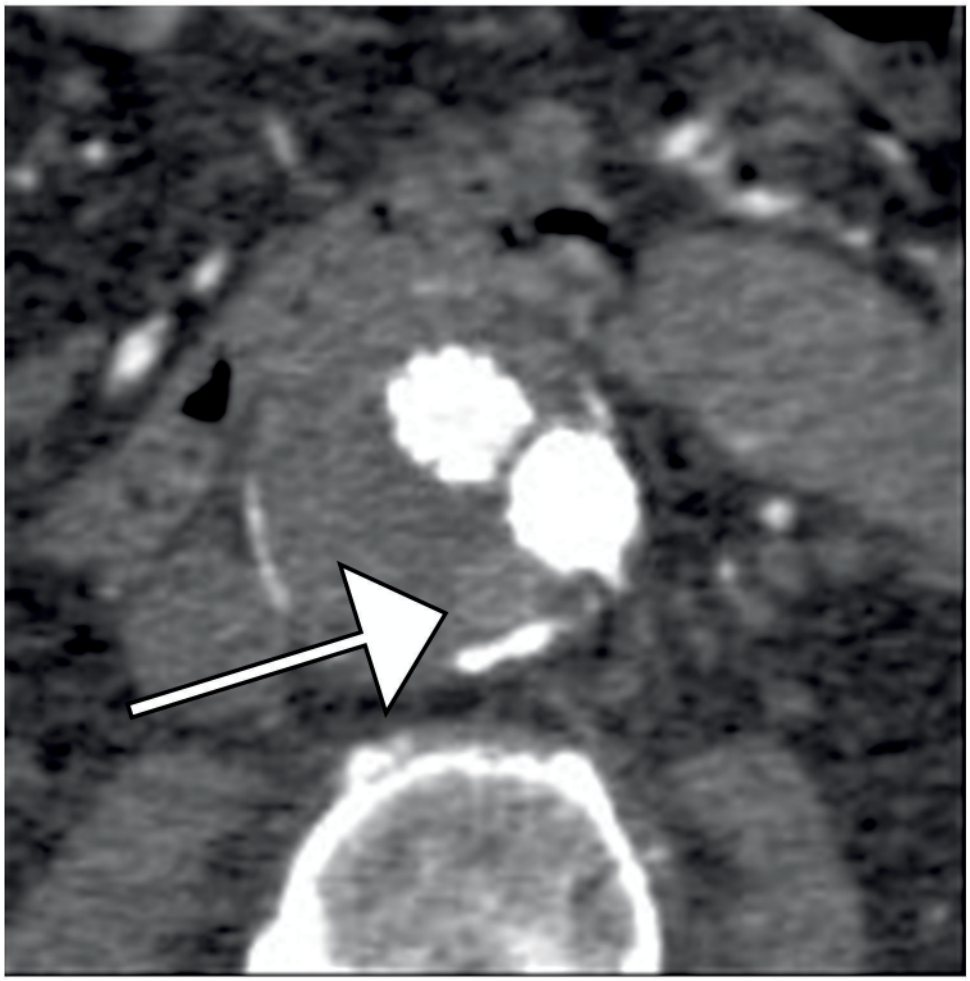

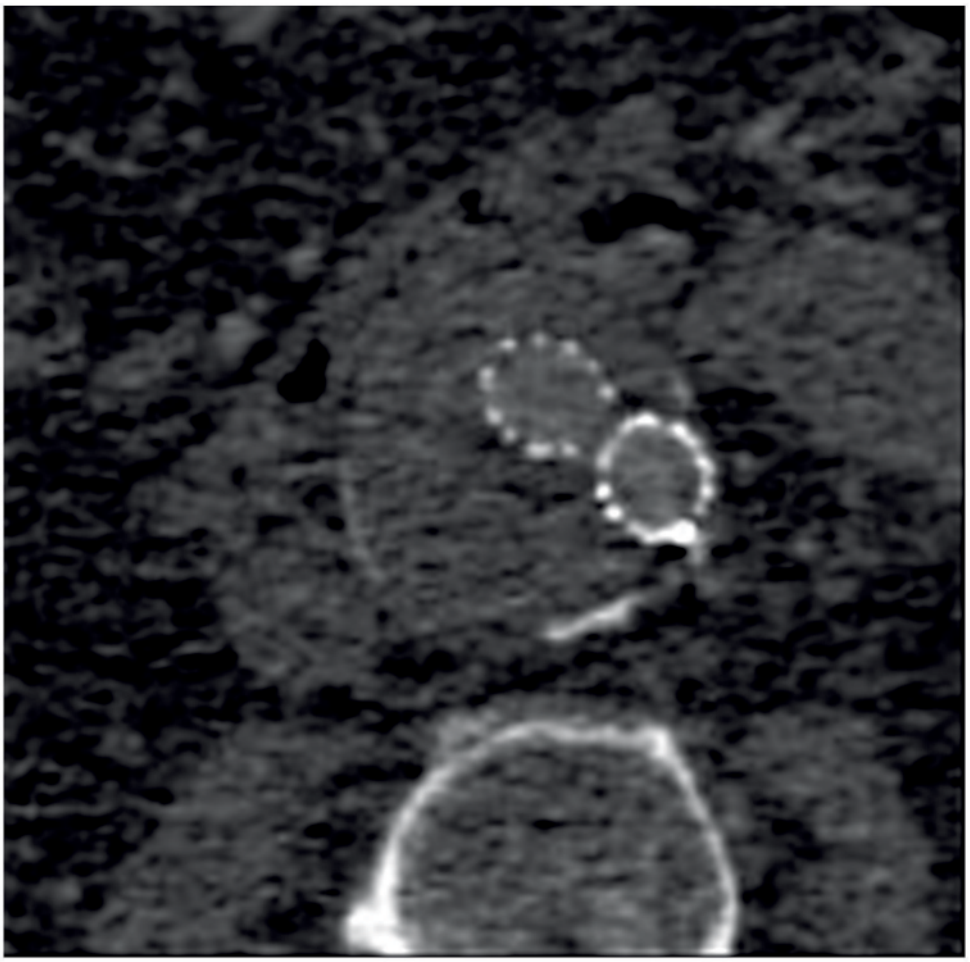

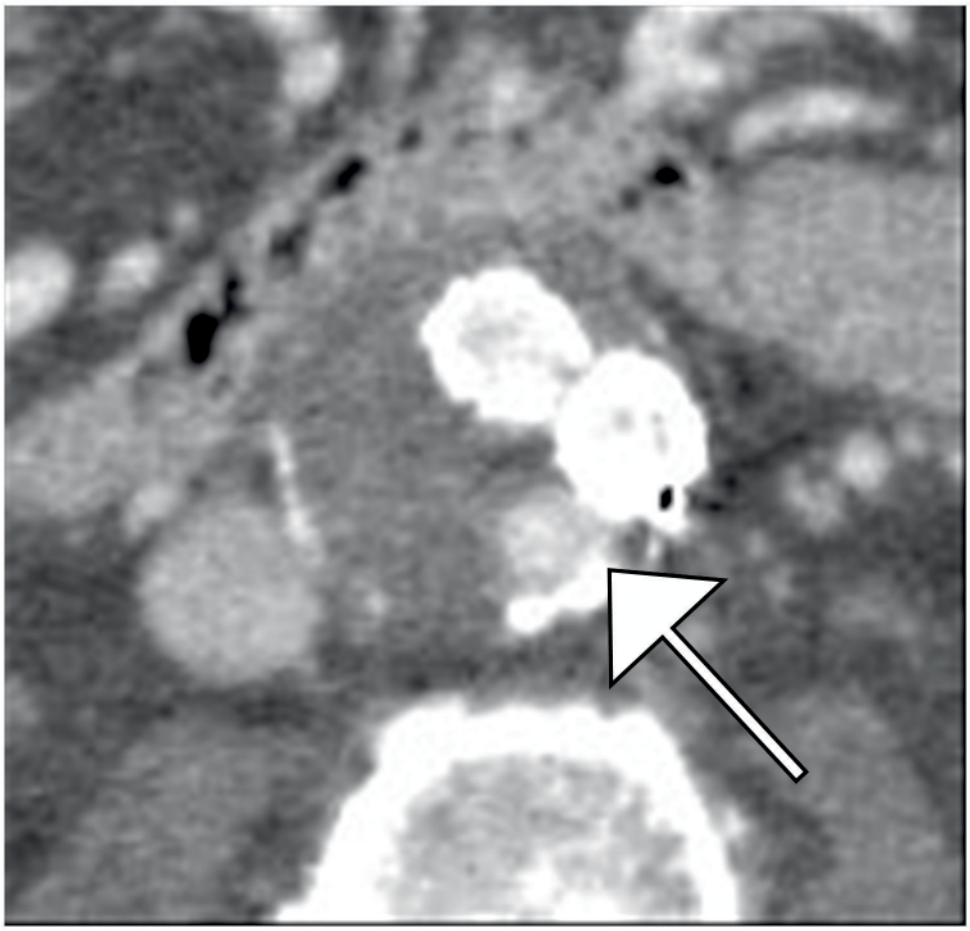

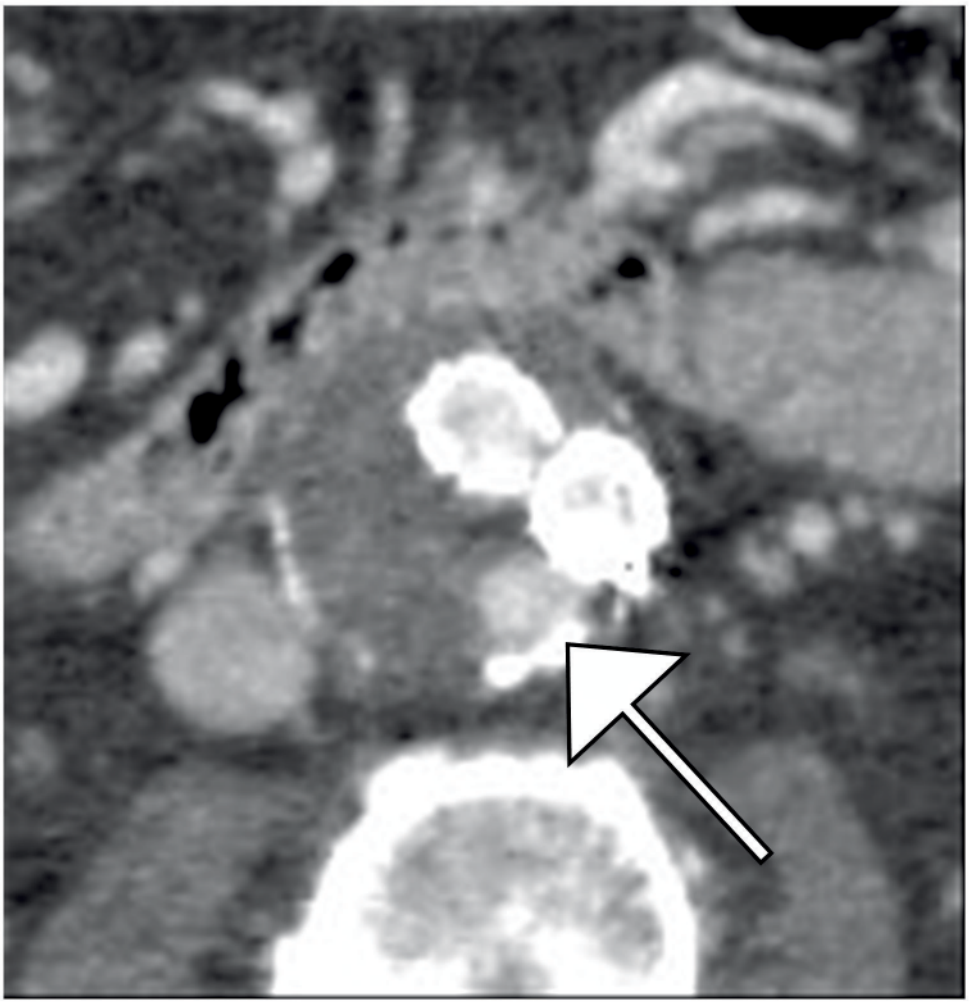

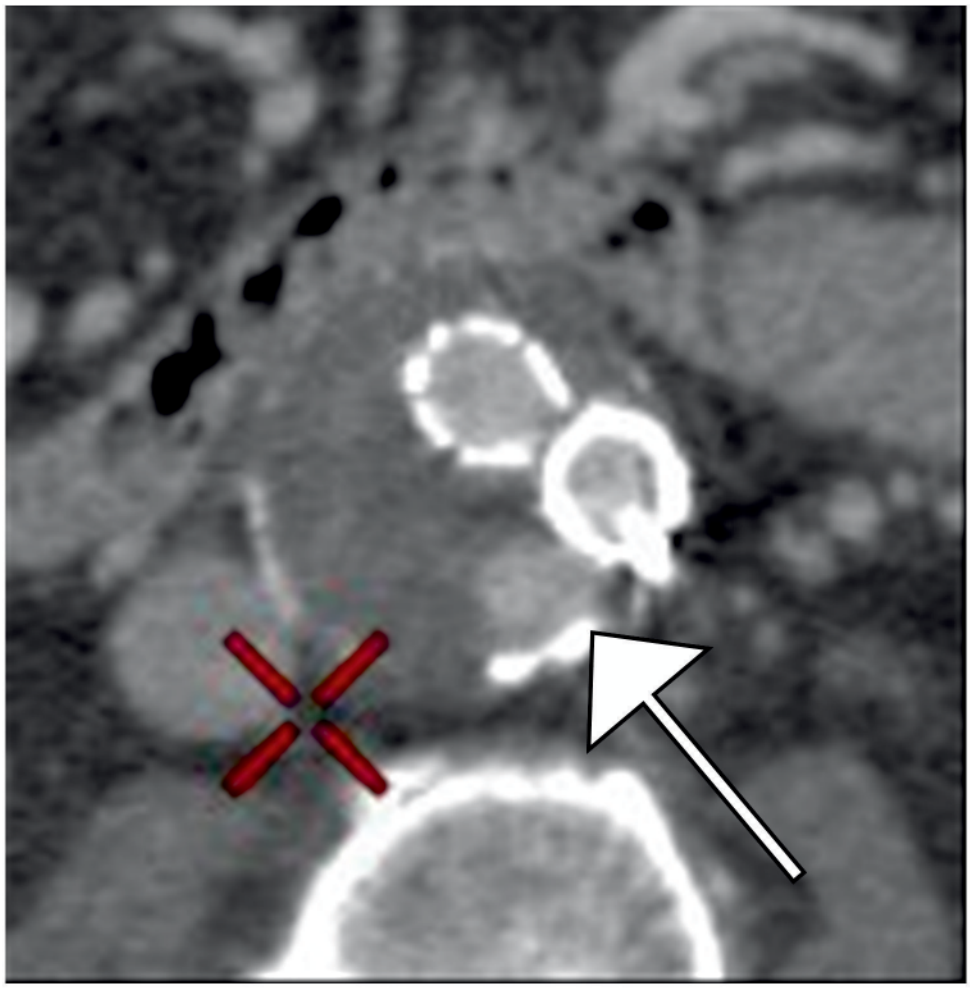

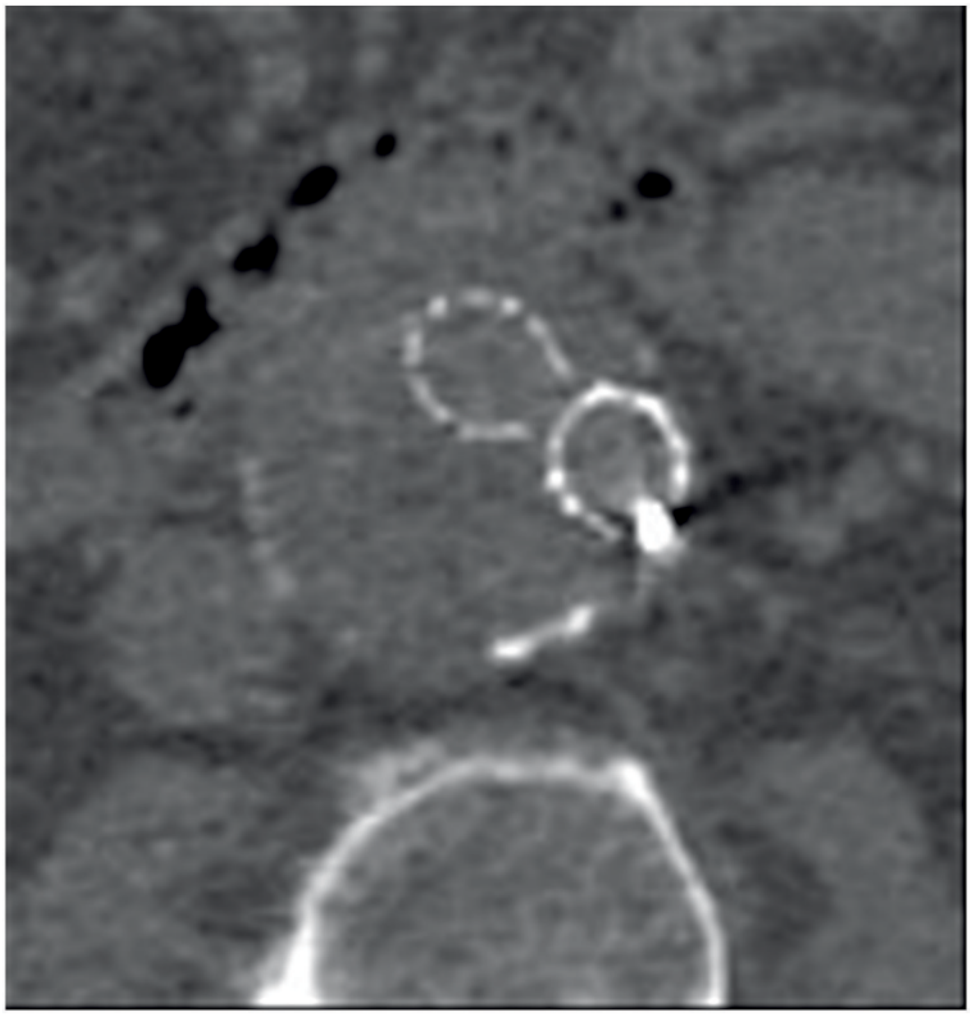

Figure 2.

80 year old man with with Type II endoleak associated with a lumbar artery. This is a single endoleak (white arrows)displayed over both phases of enhancement and multiple energy levels, demonstrating higher endoleak conspicuity at lower energy levels (A, B, E, F) and in the venous phase (E-H). The 140 keV images (D and H) show near complete disappearance of contrast within graft limbs and endoleak compared to thrombosed aneurysm sac—the probability of scatter events approaches that of diagnostic (photoelectric effect) events for iodine at this energy level.

A) 40 keV reconstruction, arterial phase
B) 55 keV reconstruction, arterial phase
C) 75 keV reconstruction, arterial phase
D) 140 keV reconstruction, arterial phase
E) 40 keV reconstruction, venous phase
F) 55 keV reconstruction, venous phase
G) 75 keV reconstruction, venous phase
H) 140 keV reconstruction, venous phase

Table 1

Reader sensitivity for leak detection

	55 keV Sensitivity (95% CI)	75 keV Sensitivity (95% CI)
Reader 1		
Overall	100.0 (82.4-100.0)	94.7 (74.0-99.9)
Arterial	63.2 (38.4-83.7)	68.4 (43.5-87.4)
Venous	100.0 (82.4-100.0)	79.0 (54.4-94.0)
Reader 2		
Overall	89.5 (66.9-98.7)	79.0 (54.4-94.0)
Arterial	63.2 (38.4-83.7)	63.2 (38.4-83.7)
Venous	84.2 (60.4-96.6)	68.4 (43.5-87.4)

CI = confidence interval

Table 2

Reader ratings of leak conspicuity where original dictation showed positive endoleak

	55 keV Mean ±SD	75 keV Mean ±SD	p-value
Overall rating			
Reader 1	5.00±0.0	4.78±0.54	*0.25*
Reader 2	4.73±0.8	4.21±1.27	***0.03***
Arterial phase			
Reader 1	3.84±1.46	3.79±1.58	*1.00*
Reader 2	3.89±1.59	3.68±1.67	*0.12*
Venous phase			
Reader 1	4.89±0.32	4.26±0.93	***0.01***
Reader 2	4.47±0.90	3.78±1.44	***0.004***